



Contents list available at IJRED website

International Journal of Renewable Energy Development

Journal homepage: <https://ijred.undip.ac.id>



Research Article

The Effect of Trailing Edge Profile Modifications to Fluid-Structure Interaction of a Vertical Axis Tidal Turbine Blade

Nu Rrhaida Arini^{a*}, Stephen R. Turnock^b, Mingyi Tan^b

^aPower Plant Engineering, Department of Mechanical Engineering and Energy, Electronic Engineering Polytechnic Institute of Surabaya, Indonesia

^bFluid Structure Interactions Group, University of Southampton, United Kingdom

Abstract. Renewable energy has become an essential energy alternative since the continual depletion of non-renewable energy resources and increasing environmental issues. Tidal energy is a promising future renewable resource which can be extracted using a vertical axis tidal turbine. Since it was proposed, a tidal turbine performance requires improvements which can be obtained by a blade's trailing edge modification. Modifying the blade's trailing edge profile is confirmed to be one way to improve a turbine's work. However, the influence of a trailing edge modifications on a vertical axis tidal turbine blade's interaction with fluid has not been fully understood. The fluid behaviour as an interaction response on a vertical axis tidal turbine blade has not been completely discovered. In this paper, 2D fluid-structure interactions of modified vertical axis tidal turbine blades are examined and modelled using OpenFOAM. The interaction exhibits fluid induced vibration which is performed by a turbine blade's displacement during operation. Three different modified blade profiles are proposed: sharp, rounded, and blunt. The modified profiles are employed to an original NACA 0012 blade and their influences on a vertical axis tidal turbine blade interaction are observed. The result discovers the fluid behaviour and fluid-induced vibrations at all positions (represented by 12 positions) over one turbine's cycle. The results demonstrate the frequency domain blade velocities and time domain blade displacements for all modified blades. The fluid behaviour around the blade is confirmed by pressure distribution plots over the blade's upper and lower surfaces. The results show that the blunt profile provides less frequent vibrations due to a reducing vorticity in the downstream fluid regime. However, the vibration amplitude that occurs on the blunt blade is higher than those of rounded and sharp profiles. Based on this research, the blunt trailing edge profile appears to be more favourable to be applied and used for vertical axis tidal turbine blades.

Keywords: Fluid-structure interactions, modified blades, fluid induced vibrations, OpenFOAM, tidal energy



@ The author(s). Published by CBIORE. This is an open access article under the CC BY-SA license (<http://creativecommons.org/licenses/by-sa/4.0/>)

Received: 9th Feb 2022; Revised: 15th April 2022; Accepted: 26th April 2022; Available online: 1st May 2022

1. Introduction

Renewable energy is a promising future energy resource to overcome fossil fuel depletion and environmental issues. Tidal energy is one of the answers for the problems. Researchers have intensively reviewed the tidal energy potency and have developed the technology to convert kinetic energy of the tides. The works which were done by Chowdhury *et al* (2021), Neil *et al* (2021), Zhou *et al* (2017), Khan *et al* (2017), Borthwick (2016), Vikas *et al* (2016), and Magagna *et al* (2015) are the examples. Borthwick (2016) reviewed the potential of offshore renewable energy or Marine Renewable Energy (MRE) including wind, tides, currents, waves, thermal and salinity. The technical potential of MRE is estimated at 16.000 TWh by 2050. Magagna *et al* (2015) emphasized the European tidal energy perspective in their study. Zhou *et al* (2017) and Khan *et al* (2017) conducted reviews in the later state. Neil *et al* (2021) updated the tidal potency around the world and discussed environmental issue which might appear in tidal energy explorations. Chowdhury *et al* (2021) predicted the increasing tidal energy exploration due to global situation

such as pandemic. In the current situation renewables might increase 1%.

The tidal energy is extracted by a tidal energy converter. Shetty and Priyam (2021) reviewed the tidal energy converter in their report. They proposed different technologies for harnessing the tidal energy across the world. One technology which can be used is a vertical axis tidal turbine (VATT). Some studies showed the advantages of vertical turbine use such as done by Khalid (2012), Eriksson *et al* (2008) and Riegler (2003). One of the main advantages come from the ability of VATT to independently operate, regardless the flow direction. Another advantage is obtained by the fatigue failure reduction, because the VATT blades are not fully facing the water flow. Since then, vertical turbines have been of interest and become a major topic in the area of renewable energy research. Researchers have focused on VATT in their studies such as done by Goesselin *et al* (2013), Brusca *et al* (2014), Almohammadi *et al* (2015), and Arini *et al* (2017). Goesselin *et al* (2013) and Brusca *et al* (2014) evaluated parametric study to design a VATT. Almohammadi *et al* (2015) and Arini *et al* (2017) proposed

* Corresponding author:
Email: arini@pens.ac.id (N.R. Arini)

a method to improve the VATT performance using a CFD method. All results showed that a VATT can be an advantageous tool to harness energy from the tide. However, the tidal turbine technology is still in immature state. The technology needs to be improved and the behaviour of the fluid when it interacts with turbines should be clearly understood to rigorously predict the turbine performance.

In this paper a Vertical Axis Tidal Turbine is studied and further improved from previous work. Since it was initially operated, the VATT technology has not been fully established yet. The fluid behaviour as a response of fluid structure interactions (FSI) of a tidal turbine has not been fully understood. Understanding the FSI clarifies the fluid behaviour on a VATT blade and is expected to regulate the fluid regime which can reduce the fluid-induced vibration (FIV) and eventually improve the turbine's performance.

One way which is confirmed to improve a turbine's performance is to modify a blade's trailing edge (TE) profile. A TE profile modification is proposed to induce fluid flow regularity in the downstream flow thus minimizing the turbulence and reducing the FIV. This paper aims to numerically investigate the fluid structure interaction of modified VATT blades by evaluating the fluid-induced vibration which is affected by the downstream fluid regime. The fluid behaviour (FSI) identification of the turbine blade is visualized at 12 locations on the circumference of a turbine rotation. The identification is executed using the CFD method. The 2D CFD models of original and modified VATT blades are developed using OpenFOAM. The design of VATT in this research employs parameters which were proposed by Goesselin *et al* (2013) and Brusca *et al* (2014). Further the evaluation of VATT performance adopts Almohammadi *et al* (2015) and Arini *et al* (2017) methods.

2. Methodology

2.1 Fluid Structure Interaction of Turbine Blades

Interactions between the turbine blades and the tides is induced by the dynamic tidal loading which mainly originates from the unsteadiness of tidal flow. The dynamic tidal loading, which is fluctuated, unpredictable, and irregular, can generate harmful vibrations on the blade structure. The vibrations may increase fatigue failure thus reduce the lifetime and raise instability problems on the structure. The risk can be minimized by understanding the behaviour of tidal flow around a tidal turbine blade and reducing the fluid induced vibration by adjusting the fluid flow to reduce the turbulence. The turbulent fluid is characterized by vortex shedding and wake generation around the blade. The objective of this research is to adjust tidal flow regime to minimize vortex generation which is expected to reduce fluid induced vibration. This will be achieved by modifying a turbine blade trailing edge profile using three different shapes. The modified trailing edge shapes are blunt, rounded, and sharp.

The dynamic loading of tides generally comes from unsteady tidal velocity which passes and rotates the turbine blades. The dynamic load generates vortex which causes the vibration on the blade. The vortex is a phenomenon when the bottom layer of fluid is rolled up and flows downward in the fluid regime. This occurs when the fluid pressure changes from stagnant pressure in the leading edge to higher pressure along the blade's surfaces. The raised pressure gradually reduces fluid velocity in the

boundary layers. The velocity discrepancy in the boundary layers, with the highest velocity in the upmost layer, creates a reverse flow and rolls the layers underneath. This forms the vortex which flow towards the trailing edge.

The vorticity as part of the actual tidal turbine response is a three-dimensional physical phenomenon of fluid structure interactions. In a numerical evaluation, a vertical axis tidal turbine model has to accommodate the turbine rotation during operation and the blade's response is caused by the interaction with the tide. This is a complicated phenomenon to model and resolve using the 3D CFD approach. There is also little experimental data provided for validation. Therefore, in this research the response model is developed in 2D using a vibrational motion to model the FSI of the blade's response. The FSI response of the blade is modelled by vibrational motion with stiffness and damping properties. The appropriate damping and stiffness constant are part of the blade structure in the 2D CFD model. Despite a structural property, the spring and damping constants of the represented blade are not detailed in this work.

In high Re flow, irregular fluid flow induces more vortex and vibrations on the tidal turbine structure. One way to overcome the vortex induced vibration is by minimizing the turbulence occurring in the flow regime. This can be done by delaying fluid separation. Modifying a blade's trailing edge shape is known to delay fluid separation. However, in an inviscid flow, the creation of layers on the blade's surfaces cannot be avoided which establish drawbacks in the flow such as velocity distribution on the surfaces. The velocity distribution generates a vortex which is explained earlier. The vortex, which is created proportionally with the Re, further sheds to the downstream and generates stronger vibrations. The strong vibration will endanger the turbine structure when the frequency is close to blade's natural frequency. In that case the lock-in frequency occurs.

Since the beginning of this century researchers studied vortex-induced vibration (VIV) and developed the understanding of this phenomenon. VIV on a simple object such as cylinder was studied by Blevins (1990). He investigated its interaction in fluid with various Re. Bishop and Hassan (1964) investigated lock-in frequency and defined it as a synchronization between natural and shedding frequency which can increase the shedding frequency thus strengthen the vibration. This happens when the shedding frequency coincides with the structure's natural frequency (lock-in). Lock-in frequency can be dangerous for a marine structure because the effect is mutually dependent, vortex induces vibrations and on the other hand stronger vibrations results in increased irregularity of the flow characteristic. Strong vibrations can cause a structure to vibrate beyond its oscillation limit. This affects the structure's performance due to its fatigue limit.

Jung and Park (2005) investigated experimentally Vortices on NACA 0012 at Re ranges from 10^4 to 10^5 . Their result showed the range of vortex shedding frequencies was influenced by angle of attack. In their oscillating angle of attack experiment, the frequency was decreased when the reduced frequency was increased. The range of frequency on the oscillating foil was also found lower than the static blade. Blade motion such as plunging, and pitching can also shed and induce vortices. The vortex generation due to combination motion was investigated to have a better concept of combination motion. Chandravanshi *et al* (2010) studied numerically a plunging

vibrating foil. The model employed NACA 0012 at Re of 10^4 in three reduced frequencies. They were 0.393, 0.785, 1.178. They found that plunge velocity and reduced frequency were important parameters wake pattern in plunging motion. Vortex on NACA 0012 with plunging and pitching motion is numerically investigated by Khalid *et al* (2014). They studied the equivalence of both motion and how it affects to vortex generation. Their result can predict the vortex shedding generation in plunging motion using pitching motion result. This can be obtained from their kinematic similarity and foil's aerodynamic performance.

2.2 Blade Modifications

In this research VATT blade modifications are employed on an original NACA 0012 blade. The turbine is designed with three blades which has 0.75 m chord length each of them and arranged symmetrically. One crucial reason for modifying an original NACA 0012 blade is because separation starts at 5° angle of attack (Mittal and Saxena, 2002). The separation creates higher fluid friction thus strengthens the drag force. The modification on the trailing edge of NACA 0012 is expected to eliminate drag force and can minimize the vortex shedding and fluid induced vibration working on a tidal turbine. This is obtained by smoothening the downstream fluid regime. Some researchers conducted numerical studies and experiments to evaluate the fluid characteristic over modified trailing edge blades such as works by Ramjee *et al.* (1986), Thompson and Whitelaw (1988), El-Gammal (2010), Gomez and Pinilla (2006), and Murcia and Pinilla (2011).

Modified NACA 0012 foil models have been developed by Ramjee *et al* (1986). Their numerical results were compared to their experiments. Their results showed that by raising the foil truncation, the value of maximum lift coefficient is improved up till the foil chord length was being cut to 15%. Beyond the truncation length, the lift coefficient was declined. The ratio of lift and drag were increased when the blade had 15% truncation and decreased if the blade was being cut off beyond that. A study of trailing edge modification to improve a foil has been done by Thompson and Whitelaw (1988). They studied the boundary layers phenomenon in the suction surfaces of sharp, blunt, and rounded trailing edge foils. His results showed the trailing edge modification generated a near wake in the downstream fluid region which lays behind trailing edge at the area within 4.5% of chord length. The near wake behind a truncated blade was also experimented by Krentel *et al* (2013). In their research the wake which was formed by 80% of chord length truncation on a blunt foil was evaluated. The results showed that the vortex at the base was formed alternatively and periodically with two pulse vortices were found at the base. A vortex emanates and alternates at lower and upper point at truncation with 180° phase shifted. Murcia and Pinilla (2011) investigated two truncation methods which was applied on NACA 4421 foils. The methods were Cutting-off and Added Thickness Methods. The Cutting-off method eliminates the rear part and rescales the blade shape from its truncated chord length. This method is adopted in this work for determining the modification of the VATT blade. The Cutting-off Method can delay stall which is expected to reduce vortex thus can eliminate vortex induced vibration.

In this research the blade modifications are blunt, rounded, and sharp trailing edge profiles. Those three modifications employ a truncation of fifteen percent

trailing edge. The final blade length is 0.6375 m. The modified trailing edge profiles are expected to smoothen the fluid flow compared to the original NACA 0012 by reducing the vorticity generation and produces longer fluid detachment on the foil surface. The blunt profile is formed by truncating the rear part of the foil by 15% of the cord length, while the sharp foil is designed by tapering the lower and upper truncated surfaces into 45° angle from the reference line. The blade chord length is considered as the reference line for the sharp formation. The rounded blade is obtained by cutting the truncated trailing edge to form a semi-circular shape. The modified blade structures are proposed to drive the vortex shedding which generates fluid induced vibration to occur far away from the natural frequencies of the blade and thus lock-in is unlikely to happen. In this paper, the VATT modified blade is further examined using 2D CFD model developed in OpenFOAM. The original and modified blade models will be detailed in Section 4.

2.3 2D CFD Tidal Turbine Blade Models

All 2D CFD models are developed in a rectangular domain for evaluating modified VATT blades using OpenFOAM. The tidal turbine is designed symmetrically for all blades. Therefore, it is assumed that on all blades identical load is produced during a turbine's rotation. This allows evaluating a VATT response model by developing a single blade rather than all blades configuration in a 2D CFD domain. With a single blade construction model, the complexity can be reduced, and the model is executed with less time.

The single blade model is developed in a rectangular domain which has $6.7c$ width and $9.8c$ length. The domain was discretized using the blockMesh utility and formed with a structured grid of quadrilateral shape. The blade is placed at $1.6c$ away from the inlet face and at the centre of the domain's width. The blade's position is closer to the domain's inlet to provide wider space in the downstream flow region to model the wake phenomenon and vorticity generation after separation near the trailing edge. The mesh in the domain which is developed using snappyHexmesh utility has seven layers with level 5 refinement over the blade's surface. The mesh has also three level grids which means, between levels, 6 adjustment cells are generated.

In OpenFOAM adjustment cells are defined as layers developed between different levels. The ratio of cell expansion is 1.3 with 0.25 to 0.7 is set as a range of layer width. The blade's spanwise length is 0.01 m which does not affect to the simulation as it is a 2D CFD model. The outlet and inlet boundaries are set to be 'patch'. The front and back boundaries are defined as 'empty' patch which accommodates a 2D model evaluation. The mesh near modified trailing edge profiles is shown in Figure 1a-1c.

The model is executed using PIMPLE algorithm which is the combination of PISO and SIMPLE algorithms. The turbulence model of $k-\omega$ SST and the Wall Function Theory in the near wall region is employed in the model. The motion response is determined by the Laplacian diffusivity equation. An additional sub-dictionary defines a restraint and a constraint for the blade motion. The direction of blade motion and axis of oscillations are assessed in the constraint parameter. The restraint parameter specifies damper and spring coefficients of the vibrating system. For the turbine rotation model, the periodic inflow equivalence concept (Arini *et al*, 2017) is applied in the model which will be explained in the Section 3.

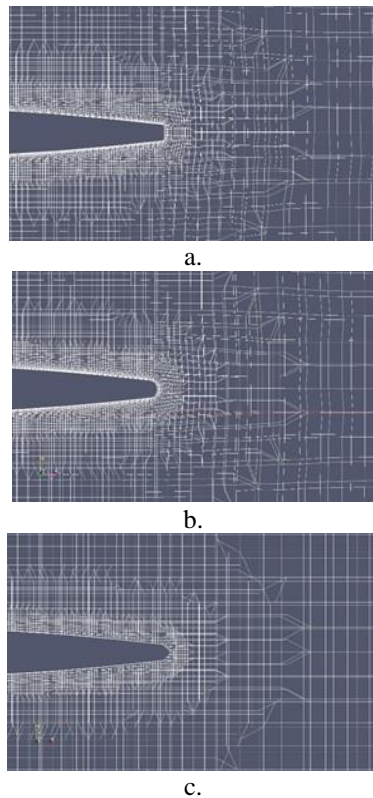


Fig. 1 Mesh around trailing edge of: a. Blunt blade, b. Rounded blade, c. Sharp blade

The blade mass is estimated from the blade material density which is selected from a composite material. Since the VATT blades works in the seawater, the blade mass calculation should also consider the added mass concept. The added mass concept has been studied by Ghassemi and Yari (2011) when they numerically studied CFD model for a turbine propeller. The influence of added mass on a hydrofoil was observed by De La Torre *et al* (2013). They developed three added mass constant modes which were associated with orientation of a foil vibration. In this research, the value for the second bending and torsion mode from De La Torre’s results are employed.

From the OpenFOAM execution, the time domain velocity at a cell which is located 0.1 m away (Jung and Park, 2005) from trailing edge is recorded. The time history velocity record is further analyzed using Phase Averaged Method, the Hilbert transform and The Power Spectral Density (PSD) to extract the frequency domain of velocity at the cell. The Phase Averaged Method which is used to analyse the dominant frequencies in this research was firstly introduced by Hussain and Reynolds (1969; 1971). The method is utilized for extracting a fluctuating signal of a coherent turbulent structure from an original signal. This method was applied by Ostermann *et al.* (2015) in their experimental study. They used the method for extracting fluctuating components from the naturally oscillating flow field. They promote the Hilbert Transform and the PSD method to further extract the vortex generation frequency. The Hilbert transform is employed to find a phase averaged signal from a reference signal. Bourgeois *et al.* (2013a; 2013b) numerically evaluated vortex shedding their foil model and discovered the Phase Average Method provided a good result in predicting vortex shedding frequency. the Phase Averaged Method was also employed by Perrin *et al.* (2006a; 2006b), They found that the method made a useful way of vortex shedding frequency prediction in their experimental study.

Table 1. Tidal Turbine design specification

Parameter	Value
Tidal Current Velocity	0.65 m/s
Tidal Density	1025 m3/kg
Dynamic Viscosity	1.03e-3 kg/m.s
Kinematic Viscosity	1.002e-6 m2/s
Tip Speed Ratio	5.1
Chord	0.75 m
Turbine diameter	1.96 m
Solidity	0.1829
Turbine aspect ratio	0.383
Blade aspect ratio	25

Jung and Park (2005) also used the Phase Averaged Method to their blade’s motion experiment to find the vortex shedding frequency. The blade’s motion in their experiment revealed an oscillating foil in an incoming flow with constant velocity. They measured the velocity of fluids using a PIV and the vortex shedding frequency was evaluated at a point which located 0.1 c from the trailing edge. The induced incoming velocity was considered as a reference signal and the signal of vortex shedding frequency was obtained. The vortex is accessed by subtracting the phase averaged velocity signal from the actual signal of the foil motion.

In this work, the Phase Averaged Method is used to determine the vortex shedding frequency. The original signals are obtained from the velocity plot. The plot is measured at a grid node which is located at 0.1 c from the trailing edge (Jung and Park 2005). Arini *et al* (2017) also used this method to examine their tidal turbine using original NACA0012. Their result will be compared to the VATT using three modified blades. The tidal turbine design characteristics are given in Table 1.

2.4. Unsteadiness of Incoming Tidal Flow

The 2D CFD model of VATT blades capture the turbine blade motion using the inertia frame of reference. This allows two motions move with different frame of reference and to model the turbine’s rotation within incoming fluid model while the blade is fixed in one position (Arini *et al*, 2017). In this way, the turbine’s blade response because of an interaction with fluid (blade’s vibration) is the only motion acting on the blade. The fluid flow is also expected to capture the unsteadiness in the incoming fluid which is assumed coming from the conversion of turbine rotation into the incoming fluid only. The turbine rotates with an angular frame of reference (R) and angular velocity ω . The inertial and rotating reference of frames have an identical origin which is the centre of VATT or turbine circular motion. Thus, a vector of any position of the rotating turbine motion can be translated in respect with inertial frame of reference as in equation (1):

$$r^{(R)} = r^{(I)}$$

Where:

$$r^{(R)} = \sum_{i=1}^2 x_i^{(R)} e_i^{(R)}$$

and

$$r^{(I)} = \sum_{i=1}^2 x_i^{(I)} e_i^{(I)}$$

Unit vector of inertial and rotating frame of references:

$$e_i^{(I)} = \text{constant}, \quad \dot{e}_i^{(R)} = \omega \times e_i^{(R)} \tag{1}$$

Both vectors act about a point on the blade with different frame of reference. The conversion of the rotating frame of reference on velocity:

$$v = \frac{d(\sum_{i=1}^2 x_i^{(I)} e_i^{(I)})}{dt} = \frac{d(\sum_{i=1}^2 x_i^{(R)} e_i^{(R)})}{dt} \tag{2}$$

The rotating frame motion can be interpreted in respect of the inertial frame of reference and the velocity equation becomes:

$$\sum_{i=1}^2 \dot{x}_i^{(I)} e_i^{(I)} = \sum_{i=1}^2 [\dot{x}_i^{(R)} e_i^{(R)} + x_i^{(R)} \dot{e}_i^{(R)}] \tag{3}$$

Substituting equation unit vector, equation (3) becomes:

$$\sum_{i=1}^2 \dot{x}_i^{(I)} e_i^{(I)} = \sum_{i=1}^2 [\dot{x}_i^{(R)} e_i^{(R)} + x_i^{(R)} (\omega \times e_i^{(R)})] \tag{4}$$

The resultant force from the tidal flow and the rotating turbine about the inertial time of reference can be derived as in Equation (5):

$$v_F^{(I)} = v_t^{(I)} + v_u^{(I)} \tag{5}$$

Substituting equation (2) to (4) into (5)

$$v_F^{(I)} = \sum_{i=1}^2 [\dot{x}_i^{(R)} e_i^{(R)} + x_i^{(R)} (\omega \times e_i^{(R)})] + x_1^{(I)} e_1^{(I)}$$

The flow in the inlet experienced by a VATT blade model is not steady. The unsteadiness is modelled by the changing angle of attack and incoming velocity magnitude in respect of inertial frame of reference. Other sources of unsteadiness are still neglected. The rotating curvilinear frame of reference employs polar coordinate. v_t and v_u becomes:

$$v_t = \dot{x}_\theta^{(R)} e_\theta^{(R)} + x_\theta^{(R)} (\omega \times e_\theta^{(R)})$$

Since

$$\dot{x}_\theta^{(R)} = 0$$

thus

$$v_t = x_\theta^{(R)} (\omega \times e_\theta^{(R)})$$

The instantaneous angle of attack (α) at all positions over a turbine rotation are determined by the periodic inflow equivalence concept which is mathematically defined and applied by Gosselin *et. al* (2013) and applied by Arini *et. al* (2017):

$$\tan \alpha = \frac{v_u^{(I)}}{v_t^{(I)} \sin x_\theta^{(R)}} + \frac{1}{\tan x_\theta^{(R)}} + x_\theta^{(R)} - \frac{\pi}{2}$$

3. Result and Discussion

The instantaneous angle of attack is a function of $x_\theta^{(R)}$ and $\dot{x}_\theta^{(R)}$. The relation can be plot as in Figures 2a and 2b. When a tidal turbine blade has zero azimuth angle and the tangential velocity is in line with the velocity of free stream, the angle of attack that works on the blade at this location is also zero thus the blade has maximum resultant velocity.

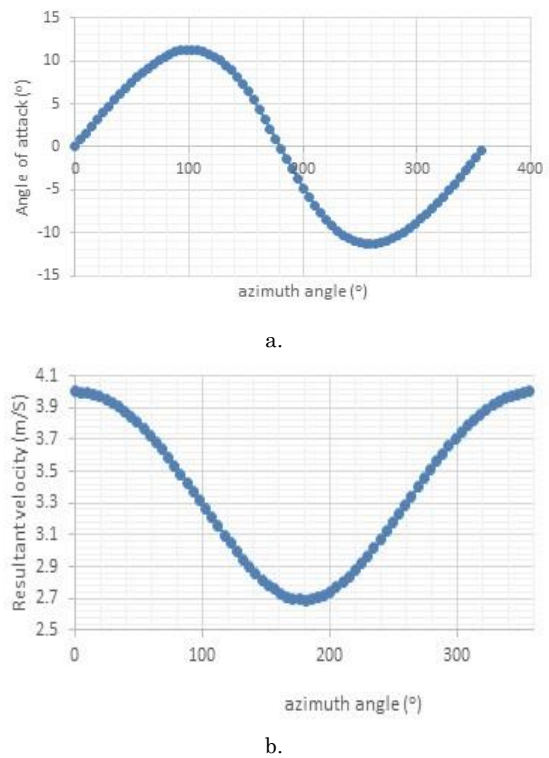


Fig. 2. a. Theoretical instantaneous angle of attack in one rotation of the turbine, b. Tidal resultant velocity

As the blade rotates and the azimuth angle increases, the blade angle of attack also increases and reduces the resultant velocity magnitude until the blade approaches azimuth angle of 90°. The angle of attack decreases from that point until it comes to azimuth angle of 180°. The maximum and minimum angle of attack are found to be 11.307° and -11.307° and occurs at 102.41° and 259.06° respectively. The range of angle of attack and the resultant velocity over a turbine rotation is depicted in Figures 3a and 3b. Both values are valid for all turbine blades regardless of the blade’s geometry and trailing edge profile. This agrees with the Goesselin *et al* (2013) study. Despite the same position angle of attack in a turbine rotation, different trailing edge shapes induce different flow behaviours and thus affects the overall pressure, forces and velocity acting on the blade’s surface. Thus, the fluid and structure interactions and blade response generation are also having different contours among the normal and modified blades although working at the same incoming fluid velocity. The blade response and interactions are performed by time domain blade displacement graphs which exhibit as fluid induced vibrations.

The influence of three trailing edge modifications on a VATT performance will be examined separately in this section. Those three results will be compared with the original NACA 0012 foil employed in a tidal turbine design (Arini *et al*, 2017) to discover the influence of each profile on a turbine’s performance. From the turbine design parameters shown in Table 1, the turbine angular velocity and turbine radius are found to be 1.71 rad/s (97.91%/s) and 1.96 m, respectively. The velocity magnitude at all azimuth angles of one rotation which is independent from trailing edge profiles, is depicted in Figure 2b. In the following discussion, the velocity magnitude for all modified blade models exhibits 3.2 repetitions which reveals the number of turbine rotations for 12 seconds simulation time (15

seconds in total with the first 3 seconds cut off to remove the transient process).

3.1. Blunt

The turbine blade utilizing a blunt trailing edge shape is firstly studied. The modification is obtained by cutting off to 15% portion of the trailing edge original foil as proposed by Ramjee *et al* (1986). The model is constructed using the mesh as shown in Figure 1a.

Figure 3a shows the velocity plots in 15 seconds omitting the first three seconds due to unsteady simulation. As seen in the figure, the velocity repeats in approximately 3.268 cycles and the profile appears to be quite regular and less chaotic. The time domain velocity is further converted to frequency domain using the Phase Averaged Method which employs the Hilbert Transform and the PSD Method as suggested by Hussain and Reynolds (1969 and 1971). Figure 3b shows the vortex shedding frequencies signal which are generated at a cell located 0,1 m away from the trailing edge as proposed by Jung and Park (2005). The signal is compared to turbine blade's natural frequency. The natural frequency is determined for transversal and rotational direction. Both natural frequencies will be compared against the vibration frequency obtained from the time domain simulation result.

From Figure 3b, it is seen that the blunt blade vibration frequencies are 0.313 Hz and 0.85 Hz. The higher response frequency is close to the blade's heave natural frequency which can amplify the blade's motion response. This implies a strong vortex induced vibration on the blade. The vibration can be examined from the displacement plot which taken at a quarter chord length point of the blade as shown in Figure 4.

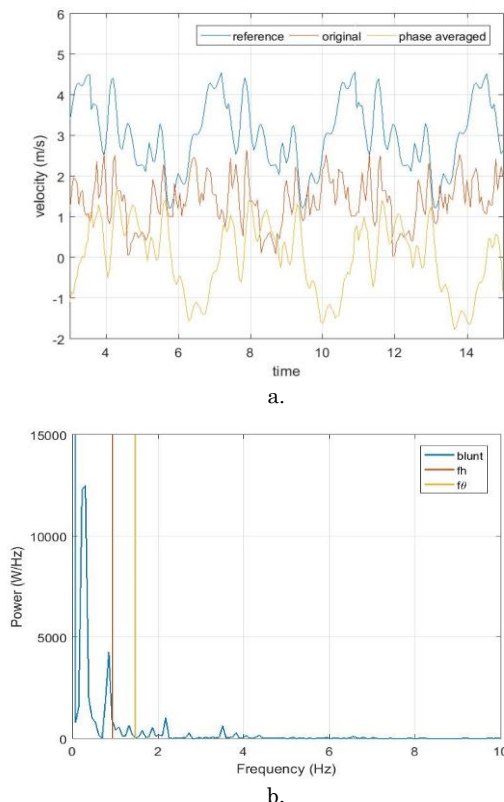


Fig. 3. Output signal for a VATT model using the blunt blade: a. time domain, b. frequency domain. (fh: heave natural frequency, fθ: pitch natural frequency)

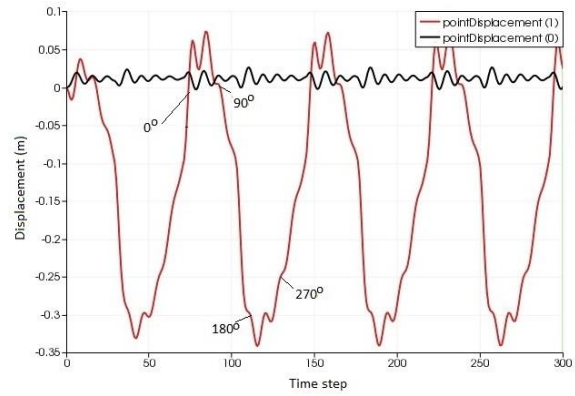


Fig. 4. Displacement for the blunt blade response

Figure 4 shows vertical (pointDisplacement 1) and horizontal (pointDisplacement 0) displacements. The pressure distribution which will verify the vortex shedding in the fluid regime over blade's surface is shown in Figure 5. Figure 6 shows the vortex generation as the response of blunt blade and fluid interaction. The vortex shedding will be detailed in regards the pressure distribution over the blade's surface.

Vortex generation begins to form at the middle of the blade at azimuth angle of 0° as shown in Figure 6. The vortex initiation is also observed from the pressure distribution plot at 0° line (red line) in Figure 5. There are two peaks at the 0° line. The peaks are located at x/c equals 0.55 and 0.33 on the upper surface. This was predicted by Blevins (1990) that the location where the vortex is shed, experience pressure oscillations. Further the vortex initiation generates small vibration which is recognized from small displacement as illustrated in the displacement plot shown in Figure 6. At this incidence, the blade is at midpoint of motion response where the vortex further moves downstream towards the trailing edge and start to detach from the blade surface.

As the blade rotates further and the azimuth angle approaches 30°, the fluid regime over the surface becomes smooth and regular as seen in Figure 6 until it reaches roughly 60° azimuth angle. From that point the vortex begins to shed and grows as it approaches 90°. The vortex generates dynamic loading and induces vibration. This indicates that the vibration working on the blade is more frequent. At 90°, both upper and lower surfaces exhibit negative pressure. This affects to suck the blades to vibrate upward as verified in the displacement plot from 0° to 90°. From that point, the blade moves to the second quarter of rotation.

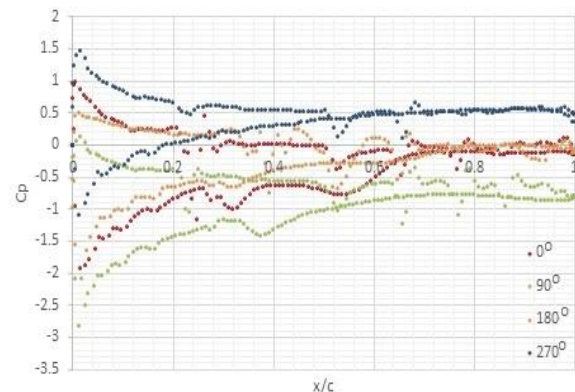


Fig. 5. Pressure distribution of a VATT model using the blunt blade at selected azimuth angles (0°,90°,180°, and 270°).

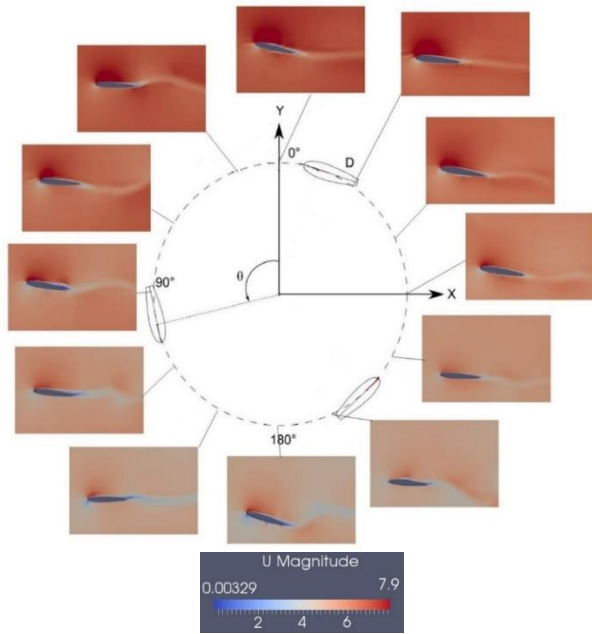


Fig. 6. Flow regime over a cycle of a turbine blade using the blunt blade.

At second quarter from the azimuth angle of 90° to 180°, the vortex is entirely detached from the blade’s upper surface. This is demonstrated by a flat pressure line (no peak) as seen in Figure 5. From 90° to 180° the total pressure is reduced which leads to reducing total force thus the blade is moved to lower position. From 180° azimuth angle, the blade rotates towards 270° azimuth angle with small vortex generation as illustrated in Figure 6. The vortex is also detected in the pressure contour plot with the presence of a small peak in Figure 5. The vortex is entirely detached and increases the pressure coefficient when approaching azimuth angle of 270°. This condition produces positive pressure on all surfaces and causes the blade to shift upwards. The smooth fluid flow regime at some positions over a turbine cycle occurred due the truncated surface on the blunt shape. This is indicated by the generation of two sources of fluid pulse recirculation behind the trailing edge. The recirculation flows prevents the regime to form a reverse fluid flow. The total displacement, which is presented by amplitude, reaches 0.3 m for a vertical axis tidal turbine using blunt shape. This maximum displacement acts in the 51.2° to 203° azimuth angle. This indicates that the blunt blade experiences strong vibrations compared to the original blade. However, the blade creates lower frequency vibration.

3.2. Rounded Foil

The mesh of vertical axis tidal turbine blade using the rounded blade is depicted in Figure 1b. The original velocity signal together with two other signals: reference and phase averaged signals are shown in Figure 7a. The PSD Method is used to convert the signal to the vortex shedding frequency which is shown in Figure 7b.

Figure 7a shows that high signal amplitude found in each turbine’s rotation. The signals are also found more chaotic. The amplitude indicates strong vibrations are working on the blade which has frequencies of 0.313 Hz and 1.1 Hz. The 1.1 Hz frequency signal is near the natural frequency on heave direction in which generates a

synchronization. The synchronization is marked by a high displacement as shown in Figure 8. The vertical axis tidal turbine with rounded blade displacement (vibration) looks like the one in blunt blade shown in Figure 6. However, the rounded blade has higher amplitude displacement than the blunt one. The vorticity is verified by the vortex generation which can be detected from the pressure distribution plot as illustrated in Figure 9. The synchronization forces the blade to proceed the heave lock-in vibration caused by vortex shedding which can be observed from the fluid behaviour image as shown in Figure 10.

From Figure 9, at azimuth angle of 0° the vortex is created on the upper surface at $x/c = 0.25$ and 0.6 which is indicated by the pressure peaks. Figure 9 also shows that the blade’s upper surface has higher total pressure than on the lower surface at the trailing edge. This creates dynamic force which induces fluid-induced vibration on the blade. The fluid induced vibration can be detected from the blade displacement at first quadrant which is illustrated in Figure 8.

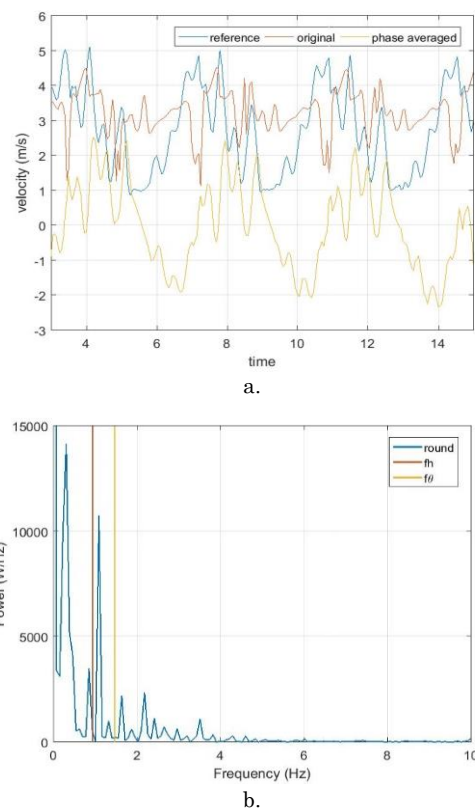


Fig. 7. Output signal for a VATT model using rounded blade: a. time domain, b. frequency domain Output (fh: heave natural frequency, fp: pitch natural frequency)

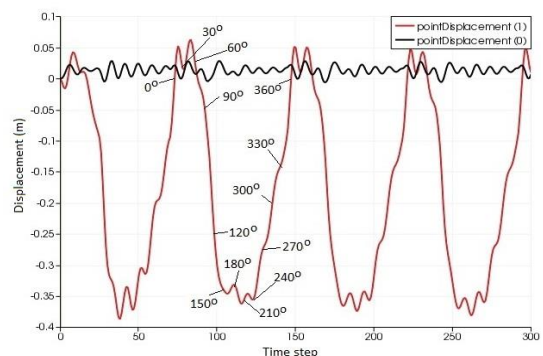


Fig. 8. Displacement for the rounded blade response

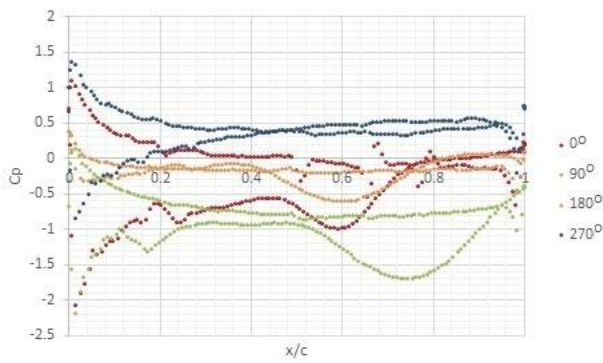


Fig. 9. Pressure distribution of a VATT model using the rounded blade at selected azimuth angles (0°, 90°, 180°, and 270°).

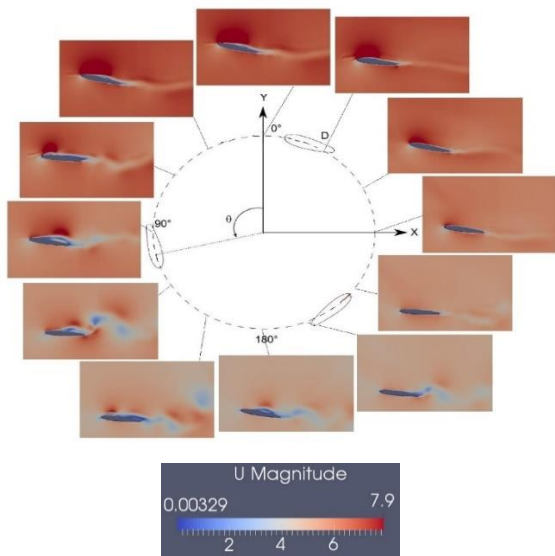


Fig. 10. Flow regime over a cycle of a turbine blade using the rounded blade.

As the blade approaches azimuth angle of 90°, the vortex grows and flows towards the trailing edge. The increasing vortex can be verified from the pressure distribution plot in Figure 9. In the 90° line (grey line) the pressure peak is found at $x/c = 0.75$. During this state, both blade surfaces have lower pressures (more negative pressures) compared to the pressure at 0° which provides a suction force to move upward. The blade vibrates in y direction with peak amplitude reaching 0.05 m away equilibrium position as indicated in the displacement plot in Figure 8.

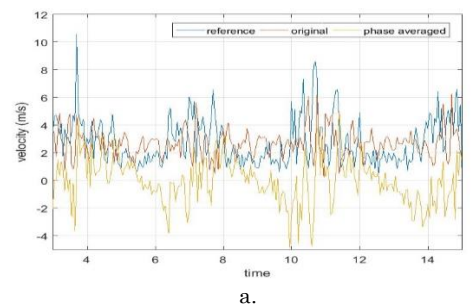
In the second quadrant section of the turbine rotation, the vortex begins to detach from at rear and flows to the downstream as remarked by vorticity in fluid flow which is highlighted in blue in Figure 10. The blade experiences higher pressure (more positive pressure) on both surfaces. This condition causes the blade to move downward as depicted in the displacement plot in Figure 8. The increasing vortex drives the blade approaching minimum position. Around azimuth angle of 180°, near the trailing edge, the total pressure of the lower surface shows lower pressure as working on the blade at 0°. Again, this generates fluctuating force which creates fluctuation/more frequent vibration as shown in Figure 10. The vibrations at 240° azimuth angle are indicated by no vortex generation and regular fluid regime at the third quadrant.

In the third quadrant, Figure 10 shows that the flow is laminar which is characterized by a fully detached vortex as seen when the blade is on 180° azimuth angle. From there, the blade moves around towards 270° with smooth flow. Both lower and upper surfaces have more positive pressure than previous quadrant. This implies that both surfaces become pressure surfaces which moves the blade to higher position as seen in Figure 8. The smooth fluid flow regime forms no fluctuation in the displacement. The blade moves from its minimum to its maximum position between 210° and 360° azimuth angle without any fluctuating motion. This can also be identified from the pressure distribution profile in Figure 9 at 270° pressure line. The line is flat and has no peak over both surfaces.

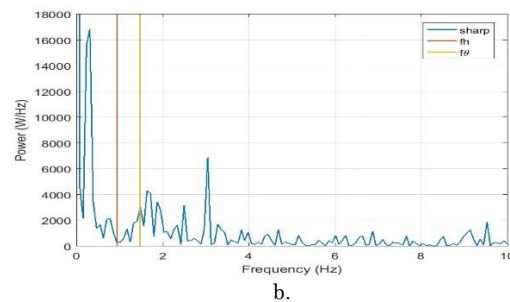
The vibration displacement between the blunt and rounded blades, as seen in Figures 4 and 8 respectively, have similar patterns although the rounded blade displacement is found to have a higher amplitude. The rounded blade vibration amplitude reaches 0.45 m which is induced by a synchronization vortex shedding frequency in respect to heave vibration. The higher amplitude displacement is also presumably caused by a higher power spectrum acting on the rounded blade. The result in agreement with Khalid *et al* (2014) which stated that the vortex can be generated by a strong heave vibration. Their numerical study showed that vortex shedding in plunging motion (heave) has equal intensity to the one occurs in pitch motion. Therefore, the rounded blade produces a more chaotic fluid flow regime than the blunt blade, though the displacement/vibration pattern of both blade profiles are similar.

3.3 Sharp Foil

The third trailing edge profile proposed is sharp which is shown in Figure 1c. The sharp blade model is generated using snappyHexMesh with similar properties to the blunt and rounded blades. The phase average signal which is obtained from the original and reference signals using the Phase Averaged Method and the Hilbert Transform is depicted in Figure 11a. Figure 11b shows the vortex shedding frequency which is calculated from the phase averaged frequency using the PSD Method.



a.



b.

Fig. 11. Output signal for a VATT model using the sharp blade: a. time domain, b. frequency domain. (fh: heave natural frequency, ff: pitch natural frequency)

Compared to the velocity signals of blunt and rounded profiles, the velocity signal for the sharp blade is more chaotic. This reflects a more chaotic fluid regime if a vertical axis tidal turbine blade employs the sharp profile. The more chaotic fluid behaviour can also be signified by the vortex shedding frequency domain plot which does not have predominant frequency in the flow as seen in Figure 11b. The plot shows that the signal peak which occurs at 0.31 Hz, lies far from the blade natural frequencies. From the same figure it is also found that the vortex sheds at higher frequencies and distracts the flow behaviour as illustrated in Figure 14. The distracted fluid regime is also explained by the vibration and pressure distribution plot which are shown in Figures 12 and 13, respectively.

In quadrant one of a turbine rotation, the vortex starts to form at leading edge as indicated by three peaks as depicted at the front part of the 0° pressure line in Figure 13. Simultaneously the previous vortex also detaches at the trailing edge as indicated by the larger peak at the trailing edge. At the upper middle part, the blade experiences more positive pressure which produces pressure fluctuations over the whole of the blade's surfaces. This reflects instability over the sharp blade which produces more frequent vibrations. The instability is also caused by alternate pressure changes over both surfaces which induces more frequent vibration. However, the total pressure is low which indicates that the blade vibration does not have high amplitude as shown in the displacement plot in Figure 12.

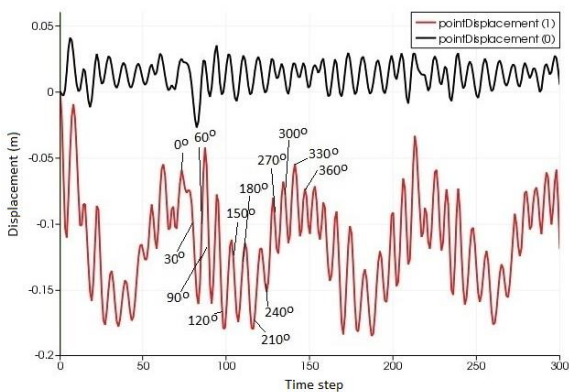


Fig. 12. Displacement for the sharp blade response

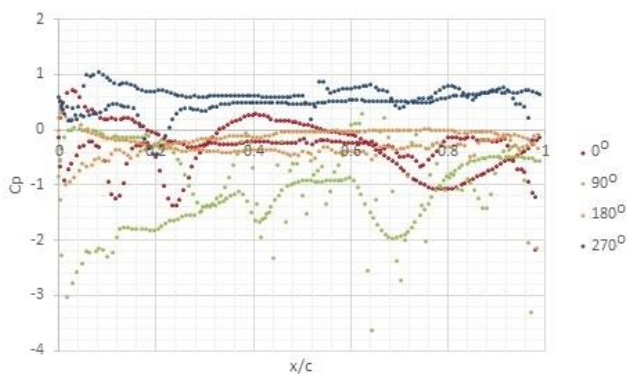


Fig. 13. Pressure distribution of a VATT model using the sharp blade at selected azimuth angles (0°, 90°, 180°, and 270°).

The leading-edge vortex at 0° azimuth angle continues to flow as remarked by the pressure peaks moving towards the trailing edge at 90° azimuth angle pressure line in Figure 13. At this point the total pressure over both surfaces is found to be more positive than when the blade at 0° azimuth angle. This demonstrates the blade has less suction pressure which moves to a lower position as shown in displacement plot in Figure 12. At 90° azimuth angle, the blade's lower surface also experiences adverse pressure gradient which generates vortex at the bottom part. The vortex is signified by a pressure peak at roughly $x/c = 0.3$. This section is also characterized by the irregular pressure which is demonstrated by a disordered pressure line on the whole lower surface. This confirms a chaotic fluid flow regime on the lower surface of the blade. From that point, the blade rotates to a position at 180° azimuth angle.

The blade moves forward to 270° azimuth angle where the pressure at both surfaces becomes positive. The leading-edge vortex generation from the second quadrant continues and moves downstream towards the trailing edge. Overall, the vortex scatters on both surfaces as seen via pressure lines in all stages in Figure 13 which is indicated by scattered peaks. The big range scattering of leading-edge vortex implies the propagation of vortices covers a wide range of shedding frequencies. From azimuth angle of 270°, the vortices is induced stronger as the blade rotates back to initial position (0°). The vortices induce vibrations on the blade which can be recognized by the turbine vibration in Figure 12. The vibration is represented by displacements measured at the blade's quarter chord length. The sharp blade vibration is more frequent compared to other modified blades due to the instability produced by the vortex generation. However, the amplitude of sharp blades is less than other modified blade's vibration due to the proximity of dominant frequencies to the blade's natural frequency occurring on the blunt and rounded blades. At the sharp blade case, the maximum displacement is found to occur at the azimuth angle of 46° and 66°. The flow regime around the sharp blade during one cycle of rotation can be seen in Figure 14

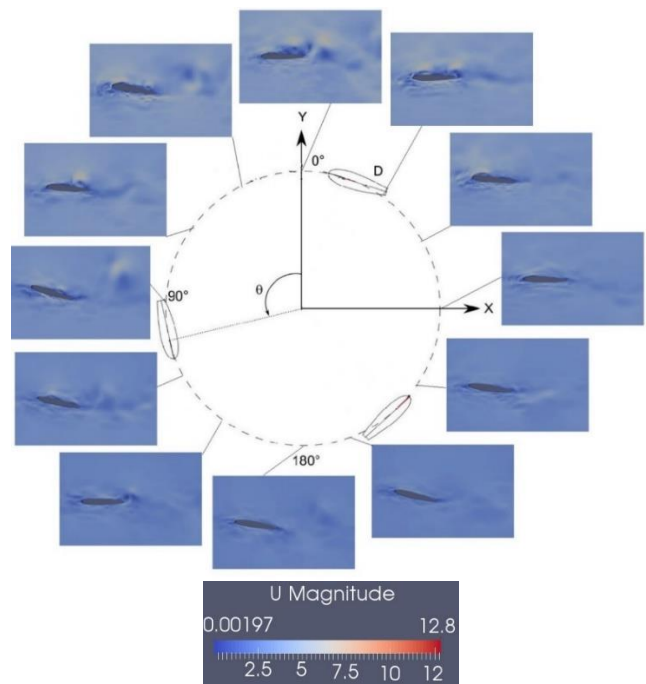


Fig. 14. Flow regime over a cycle of a turbine blade using the sharp blade.

4. Conclusion

Improvement of a vertical axis tidal turbine performance by modifying the blade's trailing edge shape is investigated numerically in this paper. Three modifications are applied in the trailing edge of NACA 0012 blade by cutting of 15% of the chord length into blunt, rounded, and sharp profiles. The model employs the equivalent incoming fluid velocity concept for modelling the unsteadiness of incoming flow. The response is observed by identifying the vortex generation behind the trailing edge, pressure distribution and blade's displacement.

The tidal turbine which employs blunt and rounded shapes experience less fluctuating displacement or vortex induce vibration. However, the sharp trailing edge profile experiences the minimum amplitude during one rotation. The rounded and blunt blades have similar vibration (displacement pattern) although the rounded blade vibrates stronger with higher amplitude. The blunt and rounded blade's vibrations have more fluctuations occurring during the first and third quadrants. Meanwhile, the sharp blade vibration is found more fluctuated in all quadrants with less amplitude. It appears the sharp blade is not suitable to be applied to a vertical axis tidal turbine as it is more unstable with more fluctuations produced by more vortex generations. The blunt and rounded blades have similar effects on the turbines. However, the blunt blade is favoured over the rounded blade to be employed at a vertical axis tidal turbine.

References

- Almohammadi, K. M., Ingham, D. B., Ma, L., and Pourkashanian, M. (2015). 2D CFD analysis of the effect of trailing edge shape on the performance of a straight-blade vertical axis wind turbine. *IEEE Transactions on Sustainable Energy*, 6(1), 228-235. DOI: [10.1109/TSSTE.2014.2365474](https://doi.org/10.1109/TSSTE.2014.2365474)
- Arini, N., Turnock, S., and Tan, M.-Y. (2018) 2D Fluid Structure Interaction Analysis Of A Vertical Axis Tidal Turbine Blade Using Periodic Inflow Equivalence Model. Accepted in Part M: *Journal of Engineering for the Maritime Environment*, Vol 232(1), 5-18. DOI: [10.1177/1475090217733843](https://doi.org/10.1177/1475090217733843)
- Bishop, R. and Hassan, A. (07-01-1964). The lift and drag forces on a circular cylinder oscillating in a flowing fluid. In *Proceedings of the Royal Society of London A: Mathematical, Physical and Engineering Sciences*, volume 277, pages 51-75. The Royal Society. DOI: <https://doi.org/10.1098/rspa.1964.0004>
- Blevins, R. D. (1977). Flow-induced vibration. *New York*.
- Borthwick, A. G. L. (2016) Marine Renewable Energy Seascape. *Engineering* 2, 69-78. DOI: <http://dx.doi.org/10.1016/J.ENG.2016.01.011>
- Bourgeois, J., Noack, B., and Martinuzzi, R. (2013a). Generalized phase average with applications to sensor-based flow estimation of the wall-mounted square cylinder wake. *Journal of Fluid Mechanics*, 736, 316-350. DOI: <https://doi.org/10.1017/jfm.2013.494>
- Bourgeois, J., Noack, B. R., and Martinuzzi, R. J. (2013b). Generalized phase averaging of experimental surface-mounted body wake measurements: 3D coherent structures & dynamical models. In TSFP DIGITAL LIBRARY ONLINE. Begel House Inc. 1-6. ISSN Online:2642-0554
- Brusca, S., Lanzafame, R., and Messina, M. (2014). Design of a vertical-axis wind turbine: how the aspect ratio affects the turbines performance. *International Journal of Energy and Environmental Engineering*, 5(4),333-340. DOI: <http://dx.doi.org/10.1007/s40095-014-0129-x>
- Chandravanshi, L. K., Chajjed, S., and Sarkar, S. (16-12-2010). Study of wake pattern behind an oscillating airfoil. In Proceeding of the 37th National & 4th International Conference on Fluid Mechanics and Fluid Power, December, pages 16-18. https://www.researchgate.net/publication/273762949_Study_of_wake_pattern_behind_an_oscillating_airfoil
- Chowdhury, M. S., Rahman, K. S., Selvanathan, V., Nuthammachot, N., Suklueng, M., Mostafaeipour, A., ... & Techato, K. (2021). Current trends and prospects of tidal energy technology. *Environment, development and sustainability*, 23(6), 8179-8194. DOI: <https://doi.org/10.1007/s10668-020-01013-4>
- Da Lozzo, E., Auricchio, F., and Calvi, G. (2012). Added mass model for vertical circular cylinder partially immersed in water. Proceedings of 15th WCEE, Lisboa. DOI: <https://paperzz.com/doc/8936219/added-mass-model-for-vertical-circular-cylinder-partially...>
- De La Torre, O., Escaler, X., Egusquiza, E., and Farhat, M. (2013). Experimental investigation of added mass effects on a hydrofoil under cavitation conditions. *Journal of Fluids and Structures*, 39,173-187. DOI: <https://doi.org/10.1016/j.jfluidstructs.2013.01.008>
- El-Gammal, M., Naughton, J., and Hangan, H. (2010). Drag force balance of a blunt and divergent trailing-edge airfoil. *Journal of Aircraft*, 47(1),345-348. DOI: <https://doi.org/10.2514/1.46308>
- Eriksson, S., Bernhoff, H., and Leijon, M. (2008). Evaluation of different turbine concepts for wind power. *Renewable and Sustainable Energy Reviews*, 12(5),1419- 1434. DOI: <https://doi.org/10.1016/j.rser.2006.05.017>
- Ghassemi, H. and Yari, E. (2011). The added mass coefficient computation of sphere, ellipsoid and marine propellers using boundary element method. *Polish Maritime Research*, 18(1),17-26. DOI: <https://doi.org/10.2478/v10012-011-0003-1>
- Goett, H. J. and Bullivant, W. K. (1939). Tests of naca 0009, 0012, and 0018 airfoils in the full-scale tunnel. National Advisory Committee for Aeronautics Report, (67). <https://digital.library.unt.edu/ark:/67531/metadc66306/>
- Gomez, A. and Pinilla, A. (2006). Aerodynamic characteristic of airfoils with blunt trailing edge. In Revista de Ingeria, pages 23-33. http://www.scielo.org.co/scielo.php?script=sci_arttext&pid=S0121-49932006000200004
- Gosselin, R., Dumas, G., and Boudreau, M. (2013). Parametric study of h-darrieus vertical-axis turbines using urans simulations. In 21st annual conference of the CFD society of Canada. DOI: <http://dx.doi.org/10.1063/1.4963240>
- Hussain, A. and Reynolds, W. (1971). The mechanics of an organized wave in turbulent shear flow. part 2. experimental results. *Journal of Fluid Mechanics*, 54(02),241|261. DOI: <https://doi.org/10.1017/S0022112072000667>
- Hussain, A. K. M. F. and Reynolds, W. C. (1969). The mechanics of an organized wave in turbulent shear flow. *Journal of Fluid Mechanics*, 41(2),241-258. DOI: <https://doi.org/10.1017/S0022112070000605>
- Jung, Y. and Park, S. (2005). Vortex-shedding characteristics in the wake of an oscillating airfoil at flow Reynolds number. *Journal of Fluids and Structures*, 20(3),451- 464. DOI: <https://doi.org/10.1016/j.jfluidstructs.2004.11.002>
- Kahn, D. L., van Dam, C., and Berg, D. E. (2008). Trailing edge modifications for flatback airfoils. technical report. institution: Sandia national laboratories. <https://www.osti.gov/servlets/purl/932882>
- Khalid, M. S. U., Akhtar, I., and Durrani, N. I. (14-10-2014). Analysis of Strouhal number-based equivalence of pitching and plunging air foils and wake deflection. Proceedings of the Institution of Mechanical Engineers, Part G: Journal of Aerospace Engineering, 229(8):1423-1434. DOI: <http://dx.doi.org/10.1177/0954410014551847>
- Khalid, S. S., Liang, Z., & Shah, N. (2012). Harnessing tidal energy using vertical axis tidal turbine. *Research Journal of Applied Sciences, Engineering and Technology*, 5(1), 239-252. <https://link.springer.com/content/pdf/10.1007/s10668-020-01013-4.pdf>
- Khan, N., Kalair, A., Abas, N., Haider, A. (2017) Review of ocean tidal, wave and thermal energy technologies. *Renewable and*

- Sustainable Energy Technologies*, 72, 590-604. DOI: <https://doi.org/10.1016/j.rser.2017.01.079>
- Krentel, D. and Nitsche, W. (2013). Investigation of the near and far wake of a bluff airfoil model with trailing edge modifications using time-resolved particle image velocimetry. *Experiments in fluids*, 54(7), 1551. DOI: <http://dx.doi.org/10.1007/s00348-013-1551-1>
- Magagna, D., & Uihlein, A. (2015). Ocean energy development in Europe: Current status and future perspectives. *International Journal of Marine Energy*, 11, 84-104. DOI: <https://doi.org/10.1016/j.ijome.2015.05.001>
- Mittal, S. and Saxena, P. (2002). Hysteresis in flow past a naca 0012 airfoil. *Computer methods in applied mechanics and engineering*, 191(19), 2207-2217. DOI: [https://doi.org/10.1016/S0045-7825\(01\)00382-6](https://doi.org/10.1016/S0045-7825(01)00382-6)
- Murcia, J. P. and Pinilla, A. (2011). CFD analysis of blunt trailing edge airfoils obtained with several modification methods. *Revista de Ingenieria*, (33), 14-24. DOI: <http://dx.doi.org/10.16924/revinge.33.2>
- Neill, S. P., Haas, K. A., Thiébot, J., & Yang, Z. (2021). A review of tidal energy—Resource, feedbacks, and environmental interactions. *Journal of Renewable and Sustainable Energy*, 13(6), 062702. DOI: [10.1063/5.0069452](https://doi.org/10.1063/5.0069452)
- OpenFOAM foundation (2017). the open source cfd toolbox user guide [openfoam. http://www.OpenFOAM.org/docs/user/tutorials.php](http://www.OpenFOAM.org/docs/user/tutorials.php). Last accessed on 02/04/2017.
- Ostermann, F., Woszidlo, R., Gaertlein, S., Nayeri, C., and Paschereit, C. O. (2015). Phase-averaging methods for a naturally oscillating flow field. In 52nd Aerospace Sciences Meeting, page 1142. DOI: <http://dx.doi.org/10.2514/6.2014-1142>
- Perrin, R., Braza, M., Cid, E., Cazin, S., Barthet, A., Sevrain, A., Mockett, C., and Thiele, F. (2006a). Obtaining phase averaged turbulence properties in the near wake of a circular cylinder at high Reynolds number using POD. *Experiments in Fluids*, 43(2-3), 341-355. DOI: <http://dx.doi.org/10.1007/s00348-007-0347-6>
- Perrin, R., Braza, M., Cid, E., Cazin, S., Moradei, F., Barthet, A., Sevrain, A., and Hoarau, Y. (2006b). Near-wake turbulence properties in the high Reynolds number incompressible flow around a circular cylinder measured by two- and three-component PIV. *Flow, turbulence and combustion*, 77(1), 185-204. DOI: <http://dx.doi.org/10.1007/s10494-006-9043-5>
- Ramjee, V., Tulapurkara, E., and Balabaskaran, V. (1986). Experimental and theoretical study of wings with blunt trailing edges. *Journal of aircraft*, 23(4), 349-352. DOI: <https://doi.org/10.2514/3.45311>
- Riegler, H. (2003). HAWT versus VAWT: Small VAWTs find a clear niche. *Refocus*, 4(4), 44-46. DOI: [https://doi.org/10.1016/S1471-0846\(03\)00433-5](https://doi.org/10.1016/S1471-0846(03)00433-5)
- Shetty, C., & Priyam, A. (2021). A review on tidal energy technologies. *Materials Today: Proceedings*. DOI: <https://doi.org/10.1016/j.matpr.2021.10.020>
- Smith, A. and Schaefer, R. F. (1950). Aerodynamics characteristic at Reynolds numbers 3×10^6 and 6×10^6 of three airfoil sections formed by cutting off various amounts from the rear portion of the NACA 0012 airfoil section. technical notes. national advisory committee for aeronautics. DOI: <http://hydrocompinc.com/wpcontent/uploads/documents/HC138-SingingPropellers.pdf>
- Standish, K., Van Dam, C. (2003). Aerodynamic analysis of blunt trailing edge airfoils. *Transactions-American Society of Mechanical Engineers Journal of Solar Energy Engineering*, 125(4), 479-487. DOI: <https://doi.org/10.1115/1.1629103>
- Thompson, B. and Whitelaw, J. (1988). Flow-around airfoils with blunt, round, and sharp trailing edges. *Journal of aircraft*, 25(4), 334-342. DOI: <https://doi.org/10.2514/3.45568>
- Uihlein, A., Magagna, D. (2016) Wave and Tidal current energy – A review of the current state of research beyond technology. DOI: <https://doi.org/10.1016/j.rser.2015.12.284>
- Vikas, M., Rao, S., & Seelam, J. K. (2016, December). Tidal energy: a review. In *Proceedings of International Conference on Hydraulics, Water Resources and Coastal Engineering (Hydro2016)*. DOI: https://www.researchgate.net/publication/310795127_Tidal_Energy_A_Review
- Zhou, Z., Benbouzid, M., Charpentier, J-F., Sculler, F. (2017) Developments in large marine current turbine technologies – A review. *Renewable and Sustainable Energy Technologies*, 71, 590-604. DOI: <https://doi.org/10.1016/j.rser.2016.12.113>

